▌**Odor Perception**

Sensory Perception of Non-Deuterated and Deuterated Organic Compounds

Tunga Salthammer,*[a] Friederike Monegel,[a] Nicole Schulz,[a] Erik Uhde,[a] Stefan Grimme,[b] Jakob Seibert,[b] Uwe Hohm,[c] and Wolf-Ulrich Palm[d]

Abstract: The chemical background of olfactory perception has been subject of intensive research, but no available model can fully explain the sense of smell. There are also inconsistent results on the role of the isotopology of molecules. In experiments with human subjects it was found that the isotope effect is weak with acetone and D_6-acetone. In contrast, clear differences were observed in the perception of octanoic acid and D_{15}-octanoic acid. Furthermore, a trained sniffer dog was initially able to distinguish between these isotopologues of octanoic acid. In chromatographic measurements, the respective deuterated molecule showed weaker interaction with a non-polar liquid phase. Quantum chemical calculations give evidence that deuterated octanoic acid binds more strongly to a model receptor than non-deuterated. In contrast, the binding of the non-deuterated molecule is stronger with acetone. The isotope effect is calculated in the framework of statistical mechanics. It results from a complicated interplay between various thermostatistical contributions to the non-covalent free binding energies and it turns out to be very molecule-specific. The vibrational terms including non-classical zero-point energies play about the same role as rotational/translational contributions and are larger than bond length effects for the differential isotope perception of odor for which general rules cannot be derived.

Introduction

The perception of smells is one of the primary instincts of humans and has always been of great social and cultural importance. Empirical studies on the composition and effects of odorous substances are known from pre-Christian times.[1] In the mid-19th century, Weber and Fechner derived a logarithmic relationship between the sense of smell and the intensity of the stimulus that triggered it. Stevens later modified the so-called Weber–Fechner law by formulating a power function.[2]

There are various theories about the mechanisms of olfactory perception and stimulation.[3] Dyson[4] considered odor receptors to be sensitive to the vibrations of molecules. Wright[5] took up this idea and correlated molecular vibrational frequencies with odor impressions. In rejection of this so-called vibration theory, Amoore[6] favored a stereo chemical approach as already presented in 1952 and postulated a classification system based on seven primary smells.[7] Wright,[8] in turn, defended his vibration theory with reference to the detailed analysis of vibration spectra of various odorants. Polak[9] assumed that odorants may have numerous mutually independent or overlapping odor active molecular profiles.

Since that time there has been an ongoing scientific debate on the question of which properties of a molecule determine its odor. Barwich[10] took this discussion as an occasion for a philosophical work on the connection between empirical success and unreliable conclusions. The structural theory was supported by Buck and Axel,[11] who identified previously unknown genes as building instructions for receptor proteins in the olfactory system. Nonetheless, Turin[12] published an extended vibration theory that explains odor perception based on the quantum mechanical tunnel effect. Brookes et al.[13] support this hypothesis on the basis of theoretical considerations.

However, Saberi and Seyed-Allaei[14] showed in experiments with Drosophila that the molecular volume influences the response of olfactory receptors. On the basis of quantitative structure–activity relationships (QSAR), Wolf et al.[15] suggest

[a] Prof. Dr. T. Salthammer, F. Monegel, N. Schulz, Dr. E. Uhde
Department of Material Analysis and Indoor Chemistry
Fraunhofer WKI, 38108 Braunschweig (Germany)
E-mail: tunga.salthammer@wki.fraunhofer.de

[b] Prof. Dr. S. Grimme, J. Seibert
Mulliken Center for Theoretical Chemistry
Institute for Physical and Theoretical Chemistry
University of Bonn, 53115 Bonn (Germany)

[c] Prof. Dr. U. Hohm
Institute of Physical and Theoretical Chemistry
University of Braunschweig—Institute of Technology
38106 Braunschweig (Germany)

[d] Dr. W.-U. Palm
Institute of Sustainable and Environmental Chemistry
Leuphana University Lüneburg, 21335 Lüneburg (Germany)

Chemistry–A European Journal

Full Paper
doi.org/10.1002/chem.202003754

Chemistry Europe
European Chemical
Societies Publishing

that human odorant detection is mainly based on the molecular shape. Genva et al.[16] mentioned that many social and cultural factors also contribute to odor perception. Sell,[17] without mentioning vibration theory, states that no generally satisfactory explanation of the mechanism of odor perception is expected in the foreseeable future. Block[3b] critically discussed different theories of olfaction and concludes that a receptor–ligand docking model best explains odor discrimination in mammals. With reference to Horsfield et al.,[18] Block[3b] suggests to name this process "docking theory of olfaction".

In the past, most theoretical studies focused on simulating an electron transfer mechanism in the first step of the olfactory response.[13, 19] These works propose a mechanism in which the molecular vibrations alter the electron transfer, resulting in a different response of the olfactory receptor (OR) with the isotopologues. Other works, however, criticize this proposal, because the electron transfer process could not be proven experimentally.[20] Another theoretical approach is the modeling of the (zero-point vibrational energy (ZPVE) induced) isotope effect on the bond lengths. In the works of Kržan et al.,[21] the hydrogen-containing bonds of the ligand (histamine as an example) are scaled by an empirical factor (based on experimental information) and differences in association energies of the complex of histamine with a model receptor are computed. The reported differences in association energies of the ligand isotopologues are caused by the elongation of the donor–acceptor intermolecular distance of the hydrogen bonds upon deuteration, known as the Ubbelohde effect.[22] The transferability of these results to the olfactory process is limited, as the interactions of odorants and OR are dominated by non-polar van der Waals interactions[23] and not by hydrogen-bonding (as investigated in the studies of Kržan et al.[21]). Furthermore, these studies compare differences in electronic energies and omit the very relevant entropic contributions to binding affinities, that is, free energies should be considered.

Our working hypothesis is that an odor molecule binds under equilibrium conditions (gas to protein-adsorbed) at various receptor proteins with different affinities leading to a molecule-specific neuronal activity pattern. No reference to other far-fetched assumptions or theories are made and only binding affinities (free association energies) similar to the case of drug–receptor binding are considered.

To understand the olfactory molecular processes it is of particular importance whether the odor perception of deuterated and non-deuterated compounds can be distinguished. The same applies to structural isomers and enantiomers.[24] The results are, however, contradictory. It is known, for example, that vanillin (4-hydroxy-3-methoxybenzaldehyde) is a strong odor compound, but isovanillin (3-hydroxy-4-methoxybenzaldehyde) can hardly be perceived in terms of smell.[25] The results regarding the olfactory distinction between (S)-(+)-carvone and (R)-(−)-carvone were inconsistent.[24] Hara[26] published that fish (Coregonus clupeaformis) can differentiate between deuterated and non-deuterated glycine. In the experiments by Haffenden et al.,[27] human subjects perceived deuterated and non-deuterated benzaldehyde differently. In contrast, Andrione et al.,[28] who used partially deuterated compounds, found that naïve

human subjects could not discriminate isotopomer pairs of 1-octanol and benzaldehyde. Further work also reports on the olfactory differentiation of deuterated and non-deuterated compounds by Periplaneta americana L.,[29] Drosophila melanogaster,[30] and Homo sapiens.[31] In contrast, Keller and Vosshall[32] found no differences in experiments with human subjects. Hoehn et al.[33] found no evidence that selective deuteration affects either the binding affinity or the activation non-olfactory G protein-coupled receptors. In the work by Muthyala et al.[34] untrained human panels were able to differentiate between the respective enantiomers of carvone and limonene, but not between deuterated and non-deuterated acetophenone. These results led to further discussions about the plausibility and implausibility of the vibration theory.[3b, 18, 20b, 35]

The sensory evaluation of construction product emissions in test chambers according to ISO 16000-28[36] stipulates the use of human subjects who are trained with acetone/air mixtures.[37] During the training sessions, the scientific question arose whether the olfactory system of these subjects can distinguish between deuterated acetone (D_6-acetone) and non-deuterated acetone. In addition, octanoic acid and D_{15}-octanoic acid were included in the studies. The latter compounds were also presented to untrained people. There was also the possibility of training a sniffer dog from the Braunschweig Police Department with octanoic acid. Then, it was examined whether the dog is able to selectively identify D_{15}-octanoic acid. We take advantage of the fact that many mammals have a highly developed sense of smell and are therefore capable of detecting and discriminating a wide spectrum of odorous molecules.[38] The experimental results are discussed considering the respective molecular properties of the compounds and on the basis of theoretical calculations.

Results and Discussion

Properties of acetone and octanoic acid

Acetone is a polar-aprotic solvent with unlimited solubility in water. At room temperature, its keto/enol tautomerization can be neglected ($pK_E = 10.3 \pm 2.0$).[39] On the completely non-polar SPB®-Octyl GC column, D_6-acetone elutes slightly earlier than acetone under isothermal conditions, which indicates a smaller hexadecane/air distribution coefficient (K_{HdA}) of D_6-acetone compared with acetone.[40] An analogous result is obtained for the slightly polar DB5 column. This shows that the octanol/air distribution coefficient (K_{OA}) is also smaller for D_6-acetone. Shi and Davis[41] found that deuterated compounds elute earlier on a DB5 column than non-deuterated compounds. Wade[42] reviewed deuterium isotope effects on non-covalent interactions between molecules and concluded that deuterated compounds are less hydrophobic than their non-deuterated isotopologues. Turowski et al. come to analogous results and explain the lower hydrophobicity of deuterated compounds with enthalpy effects.[43] The acetone odor threshold of 13900 µg m^{-3} as specified in ISO 16000-28[36] must be regarded as very unsafe, which was critically discussed by Salthammer et al.[37] Cometto-Muñiz and Abraham[44] report a considerably

Chemistry–A European Journal

Full Paper
doi.org/10.1002/chem.202003754

Chemistry
Europe
European Chemical
Societies Publishing

lower and more reliable acetone odor threshold of 832 ppb (2.0 mg m^{-3}).

With a pK_a of 4.89 (298 K), octanoic acid is one of the weaker acids. Its solubility in water is low. It can be concluded from the gas-chromatographic measurements that both the K_{HdA} and the K_{OA} for D$_{15}$-octanoic acid are smaller than for octanoic acid, the differences in retention times being significantly greater than for acetone. Comparatively few odor thresholds have been published for octanoic acid. Devos et al.[45] calculate an average of 24 µg m^{-3} from the literature. Cometto-Muñiz and Abraham[46] named an odor threshold of 0.86 ppb (5 µg m^{-3}) based on 14 responses from human subjects.

With the reference substances, the following distribution coefficients can be estimated from the gas-chromatographic measurements (see Figure S7 in the Supporting Information) using the Stenzel et al.[40a] method: logK_{HdA}(acetone) ≈ 2.0 and logK_{HdA}(octanoic acid) ≈ 4.5. For D$_{15}$-octanoic acid, the logK_{HdA} value is approximately 0.1–0.2 lower. These values correlate well with theoretical calculations (see Table S1 in the Supporting Information). The interaction with the nasal mucosa should therefore be different for deuterated and non-deuterated substances.

The role of impurities

In olfactory research, contamination of the actual target compound is a general problem, although a strict distinction must be made between chemical purity and odor purity. Even trace impurities become a problem when their odor threshold is significantly lower and the vapor pressure is significantly higher than that of the target compound.[47] Paoli et al.[48] state that investigating the selectivity of odor receptors requires gas chromatography purified odors to eliminate potential artifacts.

According to ISO 16000-28,[36] the purity of the reference compound acetone should be > 99.8 %. For the ISO standard, this may be sufficient in case of the volatile acetone with a vapor pressure of 30867 Pa (298 K).[49] For our investigations, however, we examined all substances for possible odor-related impurities by using GC-olfactometry/FID.

The GC-O/FID chromatograms are shown in the Supporting Information (Figures S9–S13). In all four experiments, the trained technical staff were only able to olfactively detect the respective target substance. In the case of acetone and D$_6$-acetone, impurities were not visible in the FID chromatogram. With octanoic acid and D$_{15}$-octanoic acid, small peaks were visible in the early retention area. However, these substances were released from the adsorbant Tenax® TA, were not relevant to odor and therefore of no importance for the experiments. Additional GC/MS analysis also gave no evidence of odor-related impurities. A small peak of γ-butyrolactone was visible in the GC/MS spectrum of D$_{15}$-octanoic acid. The odor threshold of this substance in air is not known. From the fact that the evaluators trained in GC-O/FID analysis did not correlate any odor with the corresponding FID signal, it can be concluded that γ-butyrolactone does not interfere.

Sensory assessment of octanoic acid and D$_{15}$-octanoic acid: trained subjects

The vapor pressure of octanoic acid is 0.63 Pa (298 K), which means that at room temperature only very little of the substance is released into the air. The concentrations obtained by free evaporation in the 3 m^3 stainless-steel chamber were correspondingly low (see Figure 1).

Most of the test persons were able to perceive both octanoic acid and D$_{15}$-octanoic acid, although in Experiment 1 the concentrations of 0.34–0.51 ppb were below the odor threshold given by Cometto-Muñiz and Abraham.[46]
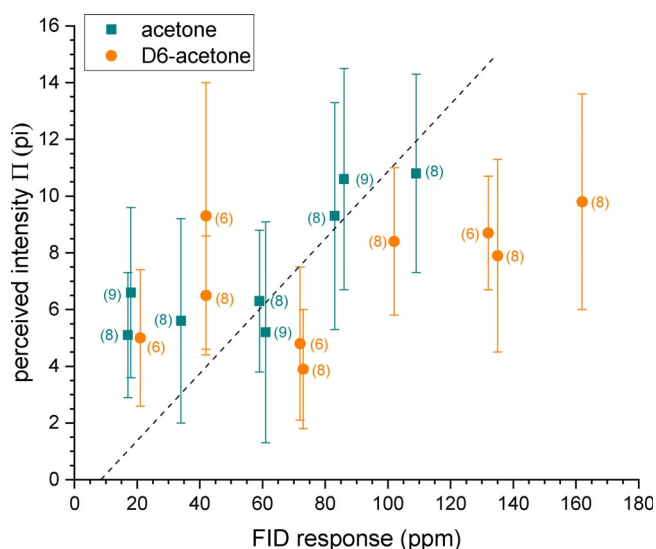
In Experiment 1, the subjects were able to differentiate between deuterated and non-deuterated octanoic acid with mean values (standard deviations) of 1.6 pi (1.2 pi) and 2.8 pi (2.7 pi). At the higher concentration of 0.51–0.86 ppb in Experiment 2, the differences were even greater with 1.7 pi (1.9 pi) and 6.1 pi (3.5 pi). For evaluation of the perceived intensity ISO 16000-28[36] requires a confidence interval CI < 2 pi at the 90 % level. This was observed in all measurements. It can therefore be concluded that the subjects perceive D$_{15}$-octanoic acid more intensely than octanoic acid at the same molar concentration.
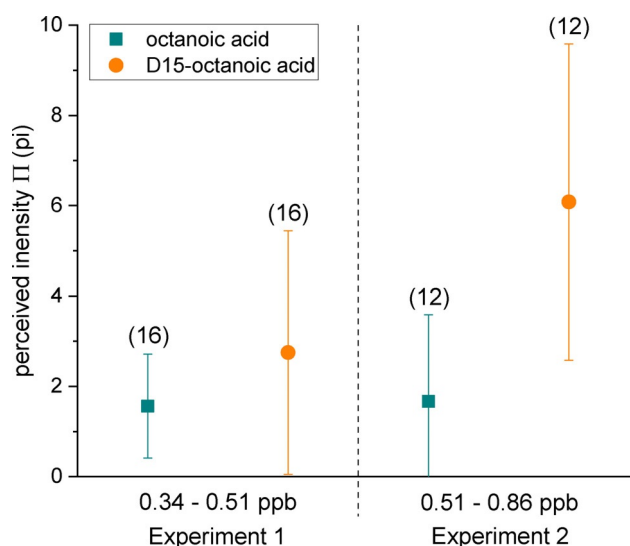
Figure 1. Odor intensity evaluation (Π-scale) of octanoic acid and D$_{15}$-octanoic acid at the 3 m^3 stainless-steel chamber by trained human subjects according to ISO 16000–28.[36] The numbers in brackets indicate the number of subjects.

Sensory assessment of acetone and D$_6$-acetone: trained subjects

A less differentiated picture emerges with acetone and D$_6$-acetone. Both substances were presented in significantly higher concentrations than the octanoic acids. Here, the trained test subjects were able to evaluate directly at the comparative scale, whereby they had to assess acetone and D$_6$-acetone in random order and concentration. The results are shown in Figure 2. First of all, it is noticeable that low concentrations in

Chemistry–A European Journal

Full Paper
doi.org/10.1002/chem.202003754

**Chemistry
Europe**
European Chemical
Societies Publishing

Figure 2. Odor intensity evaluation (Π-scale) of acetone and D_6-acetone at the comparative scale (see Figure S14 in the Supporting Information) by trained human subjects according to ISO 16000–28.[36] The numbers in brackets indicate the number of subjects and the dotted line is the ISO 16000–28 acetone calibration curve.
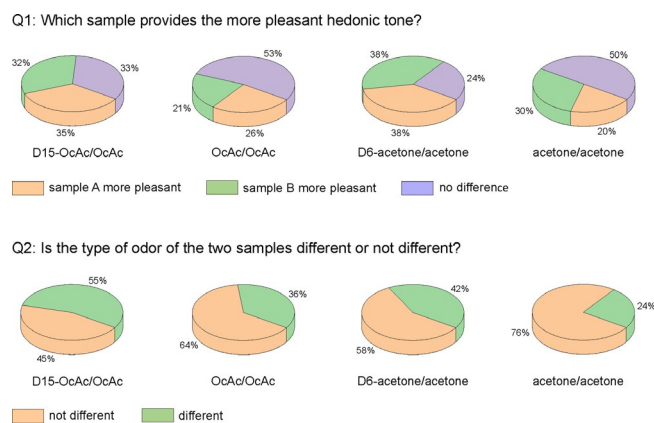

Figure 3. Results of odor evaluation of a mixed panel (trained and untrained human subjects) after presentation of the deuterated/non-deuterated compounds ($n = 69$) and non-deuterated/non-deuterated compounds ($n = 54/58$) (see also Tables S2 and S3 in the Supporting Information for details on the samples (A, B) and responses).

the range of 20–40 ppm are rated significantly higher than specified by the acetone calibration curve of ISO 16000-28. At the same time, high concentrations of D_6-acetone are rated too low. This fact has been observed and discussed previously.[37]

If the results for acetone and D_6-acetone are compared, no clear trend can be determined. Only in the middle concentration range of 60–110 ppm does D_6-acetone seem to be rated slightly higher. However, the result is not significant and means that in terms of olfactory perception, differences in intensity between acetone and D_6-acetone cannot be confirmed in this experiment.

Sensory assessment of deuterated and non-deuterated compounds: mixed panel

In further test series, the deuterated and non-deuterated substances were offered to a total of 69 trained and untrained human subjects at their respective office workplace in the Fraunhofer WKI. A control experiment was then carried out. The subjects (54–58 people each) were asked the same questions, but now two identical substances were offered from the same stock solution. The results are shown in Figure 3. Further details and information on the structure of the subject panels can be found in Tables S2 and S3 in the Supporting Information.

When the combination deuterated/non-deuterated was presented, 33% (octanoic acid) and 24% (acetone) of the subjects stated that they did not perceive any difference in hedonics. The exact question Q1 was: "which sample provides the more pleasant hedonic tone?". If differences were perceived, the answers were evenly distributed. When the combination was non-deuterated/non-deuterated, 53% (octanoic acid) and 50%

(acetone) of the subjects answered that they cannot distinguish between the two samples. Question Q2 was: "is the type of odor of the two samples different or not different?". For the combination deuterated/non-deuterated 45% (octanoic acid) and 58% (acetone) voted "not different". When the combination was non-deuterated/non-deuterated, 64% (octanoic acid) and 76% (acetone) of the subjects voted "not different".
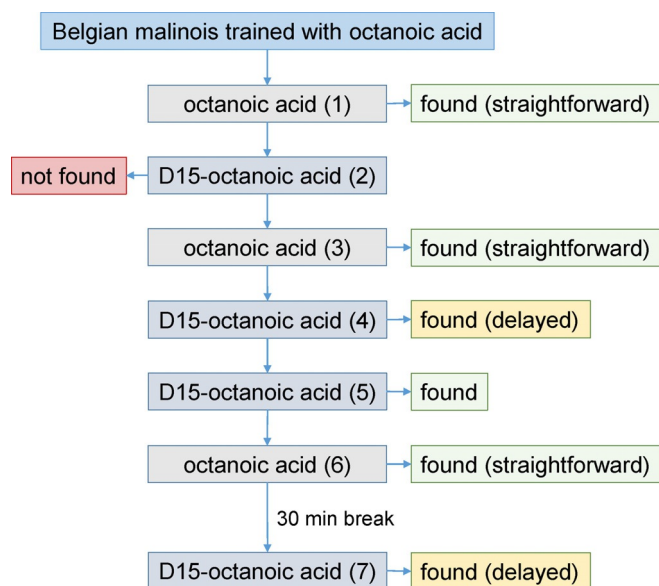
From the data evaluation, we conclude that the subjects evaluate the combinations offered differently. If the same substance is offered, the percentage of subjects who cannot differentiate is higher. Conversely, this means that the subjects perceive differences between the deuterated/non-deuterated and non-deuterated/non-deuterated combinations. According to the χ^2 test, the differences are significant at the 95% level. Nevertheless, we interpret these results as a trend. Various studies have shown that the quantitative and qualitative assessment of odor by human subjects is associated with uncertainties.[28,37,50]

Sensory assessment by a trained sniffer dog

As dogs have a particularly well-developed sense of smell, an experiment was designed to differentiate the smell of octanoic acid and D_{15}-octanoic acid with a Belgian Malinois trained for octanoic acid. It can be seen from the scheme shown in Figure 4 that the training for octanoic acid worked well.

The dog indicated the corresponding sample very quickly and in a targeted manner each time. The deuterated variant, however, was not recognized the first time. The second time, the dog hesitantly indicated the sample with D_{15}-octanoic acid, the third time even faster. After a 30 min break, the dog repeatedly hesitantly identified the D_{15}-octanoic acid as octanoic acid.

From the different reaction to octanoic acid and D_{15}-octanoic acid in Experiments 1 to 3, it becomes clear that the dog perceives the odor notes of both substances as different. The hesitant detection of D_{15}-octanoic acid in Experiment 4, howev-

Chemistry–A European Journal

Full Paper
doi.org/10.1002/chem.202003754

**Chemistry
Europe**
European Chemical
Societies Publishing

Figure 4. Results of experiments on the detection of octanoic acid and D_{15}-octanoic acid by a sniffer dog trained with octanoic acid.

er, suggests that the difference in smell is so small for the dog that after a short period of uncertainty he considers the D_{15}-octanoic acid to be octanoic acid. This behavior seems to continue as a learning effect owing to the reward after the second attempt in Experiment 5, so the D_{15}-octanoic acid is recognized as octanoic acid again. After the break, the dog again only hesitantly recognized the D_{15}-octanoic acid as octanoic acid. This confirms the assumption that there is a difference in the smell.

Theoretical strategy

The experimental results suggest that isotopologues can be perceived differently. A pure chemical structural theory is unable to explain this phenomenon. Because in the Born–Oppenheimer approximation the atomic mass does not affect the electronic structure of the odor molecule, its vibrations or the overall change of mass must influence the triggered olfactory response. If we assume that the olfactory receptor and the ligand (odor molecule) form a host–ligand complex under equilibrium conditions, standard computational techniques for computing such association free energies similar to those of supramolecular complexes or protein–drug systems[51] can be used. Such a theoretical approach has not been applied so far in our context. The molecular vibrations (and their change owing to isotopic substitution) enter thermostatistically in energetic as well as entropic contributions and, hence, a corresponding decomposition analysis seems interesting. The computed association free energy is related to the affinity of the olfactory receptor to bind a specific odorant. A strong interaction between the olfactory receptor and odor molecule should lead to a strong activation of the olfactory system and vice versa. The accurate calculation of binding/association free energies of complexes has been one of the main research areas for some of us.[52] The theoretical developments allow nowa-

days for an efficient computational treatment of large systems with biological relevance. In this work, we study small model systems as well as more realistic protein–octanoic acid complexes to shed light on the origin of the observed isotopic effect. Note, that our approach of course considers molecular vibrations as an inherent and essential part of the theoretical description but this should not be confused with Turin's vibration theory.

Quantum chemical calculations

The main quantity investigated here is the difference in association free energy ($\Delta\Delta G$) between two isotopologues given by [Eq. (1)]:
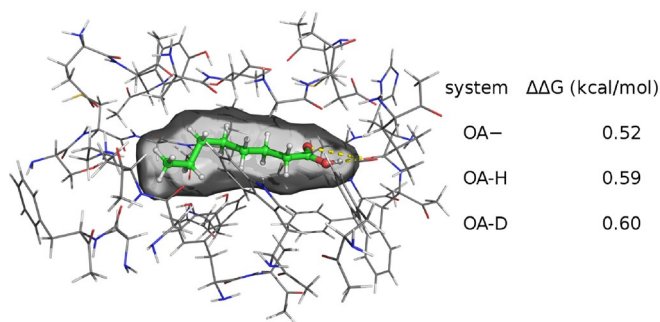
$$\Delta\Delta G = \Delta G_a^H - \Delta G_a^D \tag{1}$$

in which the superscript H/D denotes the system composed of hydrogen-only containing odorant and the corresponding isotopologue, respectively. The total association free energy of a complex (ΔG_a) is defined as [Eq. (2)]:

$$\Delta G_a = G_C - G_H - G_L \tag{2}$$

in which the indices C, H, L signify complex, host, and ligand, respectively, and G refers to the absolute molecular free energy. Further information on the quantum chemical calculation of association free energies is given in the computational details section. Positive $\Delta\Delta G$ values indicate a stronger interaction (binding) of the deuterated ligand with the host than the hydrogen containing one. This thermostatistical approach only accounts for differences in the molecular motions, but not for the mentioned isotope effect on the bond lengths (X–H bonds are effectively longer than X–D ones). Test calculations were conducted to investigate this secondary influence, showing a small contribution to $\Delta\Delta G$ of mostly < 0.1 kcal mol^{-1} ($< 10–20\%$) for larger ($>$ five carbon atoms) non-polar model systems when all CH bond lengths are strongly shortened by 2%, details of these investigations are given in the Supporting Information.

   The atomically resolved three-dimensional structure of olfactory receptors is largely unknown, but they are identified as G-protein-coupled receptors (GPCRs). A common approach is to use members of the GPCR family like bovine rhodopsin as a model.[23,53] Rhodopsin is a light-susceptible protein receptor involved in visual phototransduction that comprises the photoreactive chromophore retinal. Owing to the structural similarities between retinal and our mainly considered octanoic acid ligand, the original binding site is conserved when just the ligands are exchanged followed by reoptimization of the complexes. For reasons of computational efficiency, a cut-out for the binding site is used in the following. This structure with octanoic acid (OA) as ligand is depicted in Figure 5. The $\Delta\Delta G$ values, displayed in Figure 5, show that the complexes with deuterated OA species have significantly higher binding affinities by around 0.5–0.6 kcal mol^{-1} than the non-deuterated isotopomer. Compared with measured total binding free energies

Chemistry–A European Journal

Full Paper
doi.org/10.1002/chem.202003754

Chemistry
Europe
European Chemical
Societies Publishing

system	ΔΔG (kcal/mol)
OA−	0.52
OA-H	0.59
OA-D	0.60

Figure 5. Left: Structure of the cut-out from bovine rhodopsin as a model for an olfactory receptor with octanoic acid as ligand (odor) molecule. Right: Computed ΔΔG values for the complexes with octanoic acid as anion (OA$^-$), perdeuterated excluding carboxylic hydrogen (OA-H), and perdeuterated including carboxylic hydrogen (OA-D).

ΔG_a of typical drug molecules in typical receptors (between −5 and −15 kcal mol^{-1}),[54] this value is significant (about 3–10%). It roughly corresponds to affinity changes induced by typical chemical modifications for enhancing drug binding or effects of residue mutation in the protein and is expected to trigger the olfactory perception as observed experimentally.

The protonation state and the deuteration of the acidic hydrogen does not significantly influence ΔΔG values and for each deuteration variant of octanoic acid, the odor molecule has a higher affinity to bind in the olfactory receptor. The question if this leads in the end to a more intense and/or different odor of the isotopologue cannot be answered by the present theoretical investigation. The computed ΔΔG values for the complex of the olfactory receptor model with acetone ranges from −0.9 to −1.7 kcal mol^{-1} depending on the actual binding geometry (three were tested, see the Supporting Information for more details). The non-deuterated acetone binds stronger to the olfactory receptor than the deuterated form, which differs qualitatively from the octanoic acid cases. The observations that in the human olfactory experiments, differences between acetone isotopomers are not noticeable—in contrast to octanoic acid—cannot be explained by the present theoretical calculations, which are based on a single olfactory receptor model. This result indicates that the "true" odor perception of a compound involves much more complex mechanisms, for example, that a cascade or network of multiple receptors is involved in the olfactory process already for relatively simple molecules. Furthermore, perireceptor effects,[55] where the bioavailability of odorants is altered by enzymes in the nasal mucus before binding to ORs, could play an important role in the H/D discrimination. The theoretical assessment of this topic is, however, beyond the scope of this work. Nevertheless, the experimental and theoretical data are in qualitative agreement that a fully deuterated medium-sized organic molecule like octanoic acid can have different odor based on a physically plausible mechanism. To the best of our knowledge, this is attributed here for the first time to the thermostatistical isotope effect to total free binding energies of the odor molecule in the OR. For much smaller organic model complexes, the computed ΔΔG values are smaller and vary strongly be-

tween −0.26 and 0.04 kcal mol^{-1} (see the Supporting Information). This has prompted us to investigate the isotope effect in more detail to physically understand its mechanism. In particular, it seems interesting if ΔΔG increases monotonously with the number of deuterated positions, that is, is size extensive.

In the common rigid-rotor, harmonic-oscillator approximation (RRHO), the total ΔΔG value can be decomposed into contributions from the change of ZPVE upon binding in the different complexes (ΔΔZPVE), the corresponding enthalpy changes when going from 0 K to room temperature (ΔΔH(T)), and the changes of entropy owing to vibrational (S_{vib}), rotational (S_{rot}), and translational (S_{trans}) partition functions. The corresponding free energy contributions are depicted for three model systems in Figure 6. The ΔG_a^D values of homodimers (mixed deuterated/non-deuterated pairs) of ethylene glycol, heptane, and water were calculated. The systems were selected to cover a range of possible types of non-covalent interactions.

It is clearly seen from Figure 6 that deuteration of one of the monomers affects the individual contributions to ΔΔG similarly for all three models. The sign is negative (the deuterated system binds weaker) for the translational and rotational entropy part, as well as the thermal contributions. Conversely, the $\Delta\Delta TS_{vib}$ and zero-point vibrational energy parts consistently favor binding of the deuterated molecule. The applied level of theory (DFT or semiempirical) does not affect the contributions to a noticeable amount. The observed varying contributions of different sign and magnitude explain why sometimes a different sign for ΔΔG is obtained. We can conclude by generalizing that probably no common rule for the strength and trend of an isotope effect on odor can be derived as the various contributions may also cancel completely.

Regarding the molecule size dependence of ΔΔG, we have investigated alkane dimers from ethane to octane as models (see the Supporting Information). The values vary somewhat non-systematically from about −0.25 kcal mol^{-1} for ethane and propane to −0.08 and −0.10 kcal mol^{-1} for heptane and octane, respectively, which is in agreement with the above analysis. The negative sign of the ΔΔG values for the larger
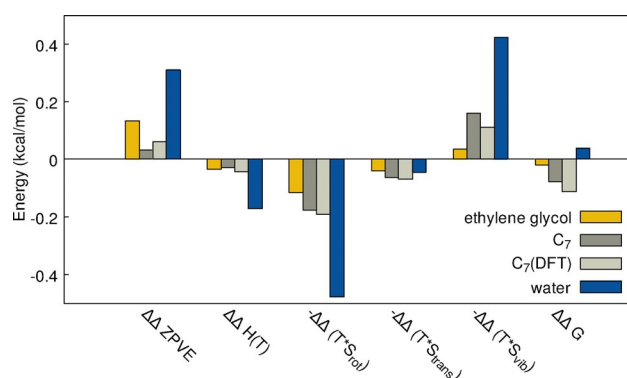
Figure 6. Decomposition of ΔΔG values into thermostatistical contributions for model dimers of ethylene glycol (orange), heptane (C$_7$, gray), and water (blue), computed with GFN2-xTB and additionally at the DFT level (B97-3c) for heptane (C7(DFT), light gray).

Chemistry–A European Journal

Full Paper
doi.org/10.1002/chem.202003754

Chemistry
Europe
European Chemical
Societies Publishing

alkane dimers (which is also confirmed by more involved DFT calculations, see the Supporting Information) indicates that binding of a non-deuterated non-polar molecule on a non-polar substrate is favored over the correspondingly deuterated one. This is qualitatively in agreement with GC experiments showing mostly shorter retention times for perdeuterated compounds (cf. Figure S8 in the Supporting Information and Wolfsberg et al.[56]), as a shorter retention time correlates with a weaker interaction of the compound with the GC matrix. This provides confidence in the reliability of our theoretical approach and the final conclusions.

Block et al.[20b] found that the responses of human and mouse olfactory receptors to deuterated and non-deuterated isotopomers of several odorants were indistinguishable. It was suggested that previously reported differences are due to peri-receptor events[55] or impurities. Na et al.,[57] who studied the response of mouse olfactory receptor neurons to deuterated and non-deuterated p-cymene, 1-octanol, 1-undecanol, and octanal, come to similar results. More than 99% of the 1610 responding neurons tested were unable to distinguish between the isotopologues. However, H/D discrimination was observed in a small percentage (0.81%) of neurons. The authors attribute this effect essentially to physical properties, for example, different hydrophobicity. Our experimental findings differ significantly from the results of Block et al.[20b] and Na et al.[57] However, according to our calculations, it is possible to explain the observed differences in odor perception of acetone and octanoic acid with the free binding energies for the interaction of the molecules with model receptors. In fact, the term 'different hydrophobicity' and different H/D binding affinities in our model mean essentially the same. Furthermore, we agree with the statements of Block et al.[20b] and Na et al.[57] that different odor and receptor responses to H and D isotopologues do not provide plausible arguments to support Turin's vibration theory of olfaction.

Tentatively, we can state that the vibrational terms ($\Delta\Delta$ZPVE and $\Delta\Delta TS_{vib}$) seem to be most system-specific but that all contributions must be considered for a quantitative description. The various free energy parts vary strongly with the type of non-covalent interaction (hydrogen vs. van der Waals bonded) and hence, the isotope effect on odor is probably very molecule-specific. Given the speed and robustness of the applied computational methods, future, more comprehensive investigations are possible. This holds true especially if well-resolved X-ray structures of olfactory receptors become available. Our investigations do not indicate major contributions to the isotope effect from C—H versus C—D bond length changes and can explain the observations without reference to an electron transfer process.

Conclusion

In nature, the sense of smell plays an outstanding role. The social and feeding behavior of most land animals is based on olfactory perception. In contrast, the sense of smell has moved into the background in everyday human life compared with seeing and hearing. In general, the molecular processes leading to the binding of an odorant to the receptor and ultimately to the triggering of the stimulus are well understood.[58] The work of Buck and Axel[11] provided an understanding of how, with the help of specific genes, odor patterns develop from individual signals, which are then passed on to the brain. On the other hand, many questions from perceptual physiology, that is, how odor stimuli are processed and interpreted in the brain, are hardly answered satisfactorily. For example, it is surprising that after a certain period of time humans adapt to unpleasant smells.[59]

The various theories on the physical and chemical background of smell perception and their sometimes-controversial arguments have already been presented. Sell[24] comments that the "shape versus vibration" debate is irrelevant as there are too many exceptions for both theories. From this point of view, we became interested in the question whether the principle olfactory differentiability of deuterated and non-deuterated compounds can shed light on the basic mechanism. We chose two prototypical model compounds for our investigations. Acetone, because many human subjects are available who are trained with this sweet-smelling substance,[37] and octanoic acid because the substance smells unpleasantly sharp at a very low odor threshold.

Under controlled conditions, the trained subjects were unable to differentiate between the odor intensity of acetone and D_6-acetone at several concentration levels. In contrast, the differences in intensity were clear and significant for octanoic acid and D_{15}-octanoic acid. The mixed panel found differences in the odor intensity for both substances in a simpler experimental setup. However, these results are not significant, as they can be influenced by saturation effects.

The dog experiment provided important results regarding the olfactory differentiation of isotopologues. The dog trained on octanoic acid was clearly unable to find D_{15}-octanoic acid on the first attempt. This shows that the odor of octanoic acid and D_{15}-octanoic acid are different. However, the dog learns quickly and already associates the odor patterns of the two isotopologues on the second and third attempt.

The quantum mechanical calculations showed a higher differential binding affinity ($\Delta\Delta G > 0$) with the model protein bovine rhodopsin for D_{15}-octanoic acid than for octanoic acid, whereby the changes in the ZPVE and the vibration entropy (S_{vib}) contribute most to the $\Delta\Delta G$ values, which are in a physically reasonable range of about 0.5–1 kcal mol^{-1} (about 10% of common drug–receptor absolute binding free energies). This example helps to explain why isotopologues of medium-sized organic molecules can have different odors. However, further calculations for acetone and other small model compounds bound to peptides (see the Supporting Information) show that general trends are lacking. The $\Delta\Delta G$ values vary depending on the chemical structure of the odor molecule and receptor and there is no clear tendency, whether the deuterated or non-deuterated complex is more stable as further indicated by a free energy decomposition analysis. In other words, it is possible that the odors of isotopomers may be perceived differently, but this is not necessarily the case.

Chemistry–A European Journal

Full Paper
doi.org/10.1002/chem.202003754

Chemistry Europe
European Chemical
Societies Publishing

In the thermostatistical analysis of calculated host–ligand total free binding energies, the vibration terms are definitely relevant. Nevertheless, our results do not support Turin's vibration theory involving an electron transfer step. To avoid confusing terminology, we would therefore like to use the wording 'vibrational thermostatistics' in corresponding discussions. In summary, the experimental and theoretical results lead us to realize that odor is a fundamental and molecule-inherent property, which cannot be explained by a single structural or energy term. We believe that this aspect should receive more attention when evaluating olfactory theories.

As pointed out by Armanino et al.,[60] "…our understanding of olfaction has evolved from simple lock-and-key models to more complex combinatorial activation of receptor ensembles". It is to be expected that the increasing efficiency of computational chemistry will lead to a significantly deeper understanding of odorant chemistry in the near future.

Experimental Section

Chemical substances

Acetone (2-propanone) (CAS 67-64-1): $\geq$ 99.9 %, picograde, LGC Standards GmbH; D_6-acetone (CAS 666-52-4): 99.9 atom % D, Sigma–Aldrich; octanoic acid (CAS 124-07-2): $\geq$ 99.5 %, analytical standard, Sigma–Aldrich; D_{15}-octanoic acid (CAS 69974-55-6): $\geq$ 98 atom % D, $\geq$ 99 % (CP), Sigma–Aldrich.

Fundamentals of ISO 16000-28

The standard ISO 16000-28 has been designed to measure the odor emission from building products in environmental test chambers using a trained sensory panel. The perceived intensity Π is determined by comparing the intensity of the sample air with different specified intensities of the reference substance acetone. The unit of Π is "pi". The comparative scale of intensity is defined as a linear acetone calibration curve $\Pi = 1/20 \times (C_{acetone} - 20)$ in the concentration range between 20 mg m^{-3} (0 pi) and 320 mg m^{-3} (15 pi). $C_{acetone}$ is the concentration in mg m^{-3}. ISO 16000-28 defines 20 mg m^{-3} as the odor threshold of acetone. A calibrated flame ionization detector (FID; Bernath Atomic, Model 3006) is used to determine the presented acetone concentration. Acetone/air mixtures in the desired concentration range were presented to the panelists via a self-designed two-diffuser device as described by Salthammer et al.[37] According to ISO 16000-28, the air volume flow through the diffuser located at the chamber must be at least 0.6 L s^{-1}. This is possible with, for example, a 3 m^3 chamber. The set air exchange must, however, then be at least 0.72 h^{-1}. Alternatively, the chamber air can be indirectly assessed after collection in containers.

Test chambers

The measurements were carried out in two different emission test chambers, which fulfill the specifications of ISO 16000-9.[61] Both chambers (3 m^3 and 4.5 m^3) were self-constructed and made of stainless steel. The chambers were set to standard operating conditions ($T = 23$ °C, 50 % relative humidity). The air exchange rate (AER) was adapted to the respective requirements.

Air sampling and chemical analysis

Sampling for the determination of octanoic acid and D_{15}-octanoic acid in the chamber air was performed by using stainless-steel tubes filled with Tenax® TA (20:35; 35:60; 300 mg). During sampling, a defined air volume of 4 L at a flow rate of 125 mL min^{-1} was passed through the collection phase. The compounds adsorbed on Tenax® were thermally desorbed (Markes TD 100) and analyzed by means of gas chromatography/mass spectrometry (Agilent 7890; TD-GC/MS). The individual substances were identified by using mass spectra (WKI database, WILEY11, NIST17) and retention time indices. All calibration standards were deposited in methanolic solution and doped on Tenax® TA.

Odor analysis was performed by using gas chromatography olfactometry coupled with flame ionization detection (GC-O/FID, Agilent 7890). The substance (0.2 μL) was spiked into a tube filled with glass wool. Cleaned air was then drawn through the tube and the organic components of this air were adsorbed on Tenax® TA. Thermal desorption took place at 300 °C (Unity 2, Markes International, UK). After separation, the gas flow was divided with a Y-splitter at the end of the GC column. One portion flowed into an olfactory detection port (ODP 3, Gerstel) and one into the FID (ratio 2:1). The sniffing of the effluent was done by trained evaluators in odor recognition via GC-O. They marked the odor active substances individually by use of voice recognition software (Dragon Natural-Speaking 10.0) and described the odor quality and intensity with basic specifications as far as it was possible. The identification of the resolved odorants was based on the odor perception, the retention index library and prevalent in comparison to data obtained by GC/MS analysis. Bartsch et al.[62] provide a detailed description of the analytical procedure.

A flame ionization detector (FID; Bernath Atomic, Model 3006) was applied for the online determination of acetone concentrations in the outlet of the diffuser at the comparative scale. The calibration procedure is described in Salthammer et al.[37] In the case of D_6-acetone, the FID signal was corrected for the molecular weight and the dissociation enthalpy of the C—D bond (see the Supporting Information). The response of an FID signal to deuterated and non-deuterated compounds has been described by Blades[63] and Holm.[64]

To examine the partitioning behavior of the deuterated and non-deuterated compounds and to estimate the hexadecane/air partitioning coefficient (K_{HdA}), gas chromatographic retention times of methanolic solutions (1 mg mL^{-1}) were determined isothermally (35 °C for acetone, 150 °C for octanoic acid) on a non-polar column (Supelco SPB®-Octyl 30 m × 250 μm × 0.25 μm) and a slightly polar column (Agilent Technologies DB-5MS UI 30 m × 250 μm × 0.25 μm), respectively. GC/MS system: Hewlett–Packard 6890 GC with 5973 MSD and Gerstel CAS3 injector; injection volume: 1 μL. Dimethyl carbonate (log$K_{HdA} = 2.24$), dimethyl sulfoxide (DMSO) (log$K_{HdA} = 3.46$), and 3-methoxy benzaldehyde (log$K_{HdA} = 5.22$) were used as reference compounds with known K_{HdA} values.[65]

Sensory assessment of octanoic acid in test chambers by trained human panels

To compare octanoic acid and D_{15}-octanoic acid, two odor evaluations were carried out with trained subjects according to ISO 16000-28 at two different concentration levels. Stainless-steel test chambers with the control settings of 23 °C and 50 % relative humidity were used.

In the first experiment, octanoic acid or D_{15}-octanoic acid (400 μL) were pipetted into an open 10 mL headspace vial and placed in a

Chemistry–A European Journal

Full Paper
doi.org/10.1002/chem.202003754

Chemistry Europe
European Chemical
Societies Publishing

$3\ m^3$ stainless-steel test chamber. The air change was set to $0.80\ h^{-1}$ to achieve the minimum air volume flow at the diffuser outlet of $0.6\ L\,s^{-1}$ for direct evaluation at the test chamber. The concentrations of octanoic acid or D_{15}-octanoic acid in the chambers of 2–$3\ \mu g\,m^{-3}$ were measured by means of TD-GC/MS.

In the second experiment, three headspace vials containing $400\ \mu L$ of substance each were placed in the test chambers. This time, a $3\ m^3$ stainless-steel chamber with an air change of $0.9\ h^{-1}$ was used for D_{15}-octanoic acid. For octanoic acid, a $4.5\ m^3$ stainless-steel chamber was used. Here, the air change was set to $0.6\ h^{-1}$, which corresponds to the same air volume flow at the diffuser outlet as for the $3\ m^3$ chamber. Concentrations of 3–$5\ \mu g\,m^{-3}$ were established in both test chambers, and the concentration was measured again by using TD-GC/MS.

Odor evaluations according to ISO 16000-28 were carried out on both doses over two days. To exclude effects regarding the sample order, octanoic acid was offered first on day one and D_{15}-octanoic acid first on day two.

Sensory assessment of acetone by trained human panels at the comparative scale

The comparative scale (see Figure S14, Supporting Information) serves to dilute gaseous acetone in a concentration range between 20–$320\ mg\,m^{-3}$. The different concentrations were offered to the test subjects via two identical diffusers made of glass. Both diffusers are continuously flushed with cleaned, humidified, and tempered air (50% relative air humidity, $T = 23\,°C$). The main air flow is divided into two equal air flows, which are fed to the two diffusers via a Y-shaped stainless-steel tube. Depending on the pi-level selected by the test subject, a certain air volume flow of the acetone/air mixture is added. Five push buttons on diffuser 1 (left) can be used to set different concentrations of non-deuterated acetone at diffuser 1. Unknown concentrations are offered at diffuser 2 (right), whereby the subjects did not know whether it was deuterated or non-deuterated acetone.

Sensory assessment of acetone and octanoic acid by a mixed human panel

To determine to what extent trained and untrained human odor perception can differentiate between deuterated and non-deuterated substances, Fraunhofer employees were asked about their odor association during the presentation of octanoic acid/D_{15}-octanoic acid (69 people), acetone/D_6-acetone (69 people), octanoic acid/octanoic acid (58 people), and acetone/acetone (54 people). In addition, personal information such as gender and age were recorded. The samples were offered to the respective survey participant one after the other in closable 10 mL glass flasks, each of the same shape and size. The quantities of odorants transferred into the flasks before the survey were $50\ \mu L$ (octanoic acid and D_{15}-octanoic acid) and $3.0\ mL$ (acetone and D_6-acetone). The surveys were carried out in the mornings between 8:30 a.m. and 12:00 a.m. Only one combination of substances (deuterated/non-deuterated) was offered per day. The subjects had the task of smelling the samples labeled A and B one after the other, memorizing the smell and then answering the following questions: a) "which sample provides the more pleasant hedonic tone?"; b) "is the type of odor of samples A and B different or not different?" Half of the subjects were initially offered the sample labeled A, the other half initially the sample labeled B.

The hedonic tone describes whether a smell is perceived as pleasant or unpleasant. According to ISO 16000-28,[36] the assessment is based on a multi-level scale. A simplified procedure was used here. The test subjects should indicate which of the samples A and B, if distinguishable, smells more pleasant.

The human subjects (trained and untrained) were fully informed about the odor experiments before the start. All tested persons have given their written consent regarding the voluntary willingness to participate in the examination program.

Sensory assessment by a trained sniffer dog

A five-year-old Belgian Malinois (at the time of the examinations) was selected, who had qualified as a protective dog by passing the annual service dog test (search, obedience, and biting exercises). In addition, owing to his pronounced play instinct, he was qualified for training as a sniffer dog (drug, explosives, fire accelerant, or corpse, blood detection dog), but was not trained as such.

An aqueous solution (500 mL) containing octanoic acid (0.1313 g) was prepared and about 150 mL of this solution was handed over to the police department. For the training, the open vial with the octanoic acid solution, together with carefully cleaned plastic tubes, was first kept in a plastic barrel that had also been cleaned. In this way, the plastic tubes took on the smell of octanoic acid. The tubes were now used regularly to play with the dog, so that the dog associated the smell with the game. In the next step, a tube was hidden in a bush. The dog had to find this first to be able to play afterwards. Finally, a piece of a plastic tube with an octanoic acid scent was cut off and placed in a clean glass jar filled with water to store the odor.[66] This glass was placed on a shelf with various compartments. The metal lid of the jar contained several holes. In the other compartments, smell samples were also prepared in glasses (water, cola, coffee, milk, ginger water, etc.). The dog's task was to find the glass with the octanoic acid, whereupon he was rewarded with playing if successful.

The sniffer dog was conditioned by trained service dog handlers in the Reiter- und Diensthundeführereinheit in der Polizeidirektion Braunschweig (rider and service dog handler squad in the Braunschweig Police Headquarters) as part of the usual and routine service dog training and in strict compliance with the German Animal Welfare Act (Tierschutzgesetz - TierSchG). The training program required for these investigations was approved by the Bezirksregierung (District Government) Braunschweig.

Computational details

If not stated otherwise, all semiempirical quantum mechanical calculations were performed at the GFN2-xTB level of theory.[67] In some cases, an included implicit solvation (GBSA) model is also applied. For the geometry optimizations and vibrational frequency calculations at the GFN2-xTB level, the xtb program (version 6.2.2) was used.[68] The ORCA[69] (version 4.2) quantum chemical package was used for all DFT calculations. For geometry optimizations and analytic frequency calculations at the DFT level, the composite method B97-3c[70] was applied. The association free energy whilst forming the complex C from molecules A and B is defined as [Eq. (3)]:

$$\Delta G_a = \Delta E + \Delta G_{RRHO}^T + \Delta G_{solv} \tag{3}$$

Here, ΔE is the gas-phase association energy, computed in the supramolecular approach [Eq. (4)]:

$$\Delta E = E_C - E_A - E_B \tag{4}$$

Chemistry–A European Journal

Full Paper
doi.org/10.1002/chem.202003754

Chemistry Europe
European Chemical
Societies Publishing

with the total quantum mechanical energy (E) of the constituents. The association free energy for a given temperature (T) includes corrections from energy to free energy in the modified rigid-rotor, harmonic-oscillator approximation (RRHO) ΔG^T_{RRHO}.[71] The ZPVE for each species in the gas phase was also added at this point. ΔG_{solv} is the difference in free solvation energy if the association occurs in the condensed phase. This contribution cancels exactly between isotopomers of the same geometrical structure in our model but may yield indirect effects by changing the geometry. The values reported in the main text include ΔG_{solv}(ether) in the structure optimizations of the protein models to embed the cut-out in an implicit protein environment, as suggested by Kržan et al.[21b] and Liao et al.[72] ΔG_{solv}(water) is included in the structure optimization of the ligand.

The geometries of the alkane dimers (C_2–C_7) are taken from the ADIM6 benchmark set.[73] The geometries of the dimers of octane (C_8), formic acid, ethylene glycol, and water were generated by the general intermolecular force field xTB-IFF.[74] The structures of the alkane and polar dimers are depicted in Figure S15 (in the Supporting Information). For the computation of ΔG_a^D, one monomer is perdeuterated, that is, the non-covalent complex consists of one hydrogen and one deuterium containing component. In the geometry optimizations, very tight convergence thresholds for the energy of 5×10^{-8} E_h and gradient norm of 5×10^{-5} E_h $Bohr^{-1}$ are applied (level extreme in xtb). For the thermostatistical calculations[71] (ΔG^T_{RRHO}), a temperature of 298.15 K was used. To address the isotope effect on the bond lengths, all deuterium containing bonds are shortened by 2% and the corresponding structures are used in the $\Delta\Delta G$ computations without further optimization. This relatively large value for the shortening is used as a definite upper limit to explore its contribution to differential H/D-binding (see, for example, Wolfsberg et al.,[56] where a value of 0.5% is mentioned).

Additionally, three neutral model peptides are generated with random amino acid residues (A: PNSIT, B: SCTYP, C: PIHDK, in single letter code) and the lowest energy conformer obtained by the CREST[75] conformational search program (see the Supporting Information). The complexes with octanoic acid and acetone are generated by the xTB-IFF and in the computation of ΔG_a^D octanoic acid/acetone is perdeuterated.

For the bovine rhodopsin, the X-ray diffraction structure 1F88[76] from the PDB[77] was used. Hydrogen atoms were added by using the maestro program,[78] resulting in a total charge of seven of the protein. The full protein was then optimized at the GFN2-xTB/GBSA level of theory. Based on this structure, a cut-out of the retinal binding pocket and adjacent residues within a 4 Å radius (including E113, G114, A117, T118, G121, E122, L125, C167, Y178, S186, C187, G188, I189, Y191, M207, F208, H211, F212, F261, W265, Y268, A269, A292, F293, A295, K296) was prepared (see Figure 5). In this cut-out, the back-bone peptides were capped with methyl groups which were placed at the peptide nitrogen atom position of the neighboring residues. The backbone C_α atoms were constrained in the GFN2-xTB/GBSA optimizations of the empty host structure and the complex with OA/acetone, respectively.

Acknowledgments

Conflict of interest

The authors declare no conflict of interest.

[1] G. Ohloff, W. Pickenhagen, P. Kraft, *Scent and Chemistry: The Molecular World of Odors*, Wiley-VCH, Weinheim, **2011**.
[2] a) S. S. Stevens, *Science* **1961**, *133*, 80 – 86; b) S. S. Stevens, *Psycholog. Rev.* **1957**, *64*, 153 – 181.
[3] a) A. Sharma, R. Kumar, I. Aier, R. Semwal, P. Tyagi, P. Varadwaj, *Current Neuropharmacol.* **2019**, *17*, 891 – 911; b) E. Block, *J. Agric. Food Chem.* **2018**, *66*, 13346 – 13366.
[4] G. Malcolm Dyson, *J. Soc. Chem. Ind.* **1938**, *57*, 647 – 651.
[5] R. H. Wright, *J. Appl. Chem.* **2007**, *4*, 611 – 615.
[6] J. E. Amoore, *Nature* **1963**, *198*, 271 – 272.
[7] J. E. Amoore, *Nature* **1967**, *214*, 1095 – 1098.
[8] R. H. Wright, *Nature* **1966**, *209*, 571 – 573.
[9] E. H. Polak, *J. Theoret. Biol.* **1973**, *40*, 469 – 484.
[10] A.-S. Barwich, *Studies in History and Philosophy of Science Part A* **2018**, *69*, 40 – 51.
[11] L. Buck, R. Axel, *Cell* **1991**, *65*, 175 – 187.
[12] a) L. Turin, *Chem. Senses* **1996**, *21*, 773 – 791; b) L. Turin, *J. Theoret. Biol.* **2002**, *216*, 367 – 385.
[13] J. C. Brookes, F. Hartoutsiou, A. P. Horsfield, A. M. Stoneham, *Phys. Rev. Lett.* **2007**, *98*, 038101.
[14] M. Saberi, H. Seyed-Allaei, *Sci. Rep.* **2016**, *6*, 25103.
[15] S. Wolf, L. Gelis, S. Dörrich, H. Hatt, P. Kraft, *PLoS One* **2017**, *12*, e0182147.
[16] M. Genva, M. Deleu, L. Lins, M.-L. Fauconnier, *Int. J. Mol. Sci.* **2019**, *20*, 3018.
[17] C. S. Sell, *Angew. Chem. Int. Ed.* **2006**, *45*, 6254 – 6261; *Angew. Chem.* **2006**, *118*, 6402 – 6410.
[18] A. P. Horsfield, A. Haase, L. Turin, *Adv. Physics: X* **2017**, *2*, 937 – 977.
[19] a) E. R. Bittner, A. Madalan, A. Czader, G. Roman, *J. Chem. Phys.* **2012**, *137*, 22A551; b) I. A. Solov'yov, P. Y. Chang, K. Schulten, *Phys. Chem. Chem. Phys.* **2012**, *14*, 13861 – 13871; c) A. Chęcińska, F. A. Pollock, L. Heaney, A. Nazir, *J. Chem. Phys.* **2015**, *142*, 025102.
[20] a) E. Block, S. Jang, H. Matsunami, V. S. Batista, H. Zhuang, *Proc. Natl. Acad. Sci. USA* **2015**, *112*, E3155 – E3155; b) E. Block, S. Jang, H. Matsunami, S. Sekharan, B. Dethier, M. Z. Ertem, S. Gundala, Y. Pan, S. Li, Z. Li, S. N. Lodge, M. Ozbil, H. Jiang, S. F. Penalba, V. S. Batista, H. Zhuang, *Proc. Natl. Acad. Sci. USA* **2015**, *112*, E2766 – E2774.
[21] a) M. Kržan, J. Keuschler, J. Mavri, R. Vianello, *Biomolecules* **2020**, *10*, 2 – 11; b) M. Kržan, R. Vianello, A. Maršavelski, M. Repič, M. Zakšek, K. Kotnik, E. Fijan, J. Mavri, *PLoS ONE* **2016**, *11*, e0154002.
[22] A. R. Ubbelohde, K. J. Gallagher, *Acta Crystallogr.* **1955**, *8*, 71 – 83.
[23] S. Katada, T. Hirokawa, Y. Oka, M. Suwa, K. Touhara, *J. Neurosci.* **2005**, *25*, 1806 – 1815.
[24] C. S. Sell, *Chemistry and the Sense of Smell*, Wiley, Hoboken, **2014**.
[25] T. Egawa, A. Kameyama, H. Takeuchi, *J. Mol. Struct.* **2006**, *794*, 92 – 102.
[26] J. Hara, *Experientia* **1977**, *33*, 618 – 619.
[27] L. J. W. Haffenden, V. A. Yaylayan, J. Fortin, *Food Chem.* **2001**, *73*, 67 – 72.
[28] M. Andrione, M. Paoli, R. Antolini, A. Haase, *J. Biol. Res.* **2017**, *37*, 56 – 60.
[29] B. R. Havens, C. E. Meloan, *Dev. Food Sci.* **1995**, *37*, 497 – 524.
[30] M. I. Franco, L. Turin, A. Mershin, E. M. C. Skoulakis, *Proc. Natl. Acad. Sci. USA* **2011**, *108*, 3797 – 3802.
[31] S. Gane, D. Georganakis, K. Maniati, M. Vamvakias, N. Ragoussis, E. M. C. Skoulakis, L. Turin, *PLoS ONE* **2013**, *8*, e55780.
[32] A. Keller, L. B. Vosshall, *Nat. Neurosci.* **2004**, *7*, 337 – 338.
[33] R. D. Hoehn, D. E. Nichols, J. D. McCorvy, H. Neven, S. Kais, *Proc. Natl. Acad. Sci. USA* **2017**, *114*, 5595 – 5600.

[34] R. S. Muthyala, D. Butani, M. Nelson, K. Tran, *J. Chem. Educ.* **2017**, *94*, 1352–1356.

[35] a) L. B. Vosshall, *Proc. Natl. Acad. Sci. USA* **2015**, *112*, 6525–6526; b) L. Turin, S. Gane, D. Georganakis, K. Maniati, E. M. C. Skoulakis, *Proc. Natl. Acad. Sci. USA* **2015**, *112*, E3154; c) R. D. Hoehn, D. E. Nichols, H. Neven, S. Kais, *Frontiers Phys.* **2018**, *6*, 25.

[36] ISO 16000–28, Indoor Air—Part 28: Determination of odour emissions from building products using test chambers, Beuth, Berlin, **2012**.

[37] T. Salthammer, N. Schulz, R. Stolte, E. Uhde, *Indoor Air* **2016**, *26*, 796–805.

[38] a) H. Kida, Y. Fukutani, J. Mainland, C. de March, A. Vihani, A. Toyama, L. Liu, M. Kameda, M. Yohda, H. Matsunami, *Nat. Commun.* **2018**, *9*, 4556; b) X. S. Hu, K. Ikegami, A. Vihani, K. W. Zhu, M. Zapata, C. A. de March, M. Do, N. Vaidya, G. Kucera, C. Bock, Y. Jiang, M. Yohda, H. Matsunami, *eNeuro* **2020**, *7*, ENEURO.0103-19.2019.

[39] Y. Chiang, A. J. Kresge, N. P. Schepp, *J. Am. Chem. Soc.* **1989**, *111*, 3977–3980.

[40] a) A. Stenzel, S. Endo, K.-U. Goss, *J. Chromatogr. A* **2012**, *1220*, 132–142; b) N. Ulrich, S. Endo, T. N. Brown, N. Watanabe, G. Bronner, M. H. Abraham, K.-U. Goss in *UFZ-LSER database vol. 3.2.1 [Internet]*, Helmholtz Centre for Environmental Research, Leipzig, **2017**.

[41] B. Shi, B. H. Davis, *J. Chromatography A* **1993**, *654*, 319–325.

[42] D. Wade, *Chemico-Biological Interactions* **1999**, *117*, 191–217.

[43] M. Turowski, N. Yamakawa, J. Meller, K. Kimata, T. Ikegami, K. Hosoya, N. Tanaka, E. R. Thornton, *J. Am. Chem. Soc.* **2003**, *125*, 13836–13849.

[44] J. E. Cometto-Muñiz, M. H. Abraham, *Behavioural Brain Res.* **2009**, *201*, 207–215.

[45] M. Devos, F. Patte, J. Rouault, P. Laffort, L. J. Van Gemert, *Standardized Human Olfactory Thresholds*, Oxford University Press, Oxford, **1992**.

[46] J. E. Cometto-Muñiz, M. H. Abraham, *Exper. Brain Res.* **2010**, *207*, 75–84.

[47] D. L. P. Schorkopf, B. P. Molnár, M. Solum, M. C. Larsson, J. G. Millar, Z. Kárpáti, T. Dekker, *Progress in Neurobiol.* **2019**, *181*, 101661.

[48] M. Paoli, D. Munch, A. Haase, E. Skoulakis, L. Turin, C. G. Galizia, *Eneuro* **2017**, *4*, ENEURO.0070-17.2017.

[49] D. Ambrose, C. H. S. Sprake, R. Townsend, *J. Chem. Thermodyn.* **1974**, *6*, 693–700.

[50] T. Salthammer, N. Schulz, R. Stolte, F. Monegel, E. Uhde, *Building and Environment* **2020**, *172*, 106668.

[51] a) R. Sure, S. Grimme, *J. Chem. Theory Comput.* **2015**, *11*, 3785–3801; b) S. Ehrlich, A. H. Göller, S. Grimme, *ChemPhysChem* **2017**, *18*, 898–905.

[52] a) R. Sure, J. Antony, S. Grimme, *J. Phys. Chem. B* **2014**, *118*, 3431–3440; b) J. Antony, R. Sure, S. Grimme, *Chem. Commun.* **2015**, *51*, 1764–1774; c) R. Sure, S. Grimme, *Chem. Commun.* **2016**, *52*, 9893–9896; d) F. Bohle, S. Grimme, *J. Serb. Chem. Soc.* **2019**, *84*, 837–844; e) J. L. Kuo, T. Gunasekara, A. Hansen, H. B. Vibbert, F. Bohle, J. R. Norton, S. Grimme, P. J. Quinlivan, *Organometallics* **2019**, *38*, 4319–4328; f) S. Oswald, N. A. Seifert, F. Bohle, M. Gawrilow, S. Grimme, W. Jäger, Y. Xu, M. A. Suhm, *Angew. Chem. Int. Ed.* **2019**, *58*, 5080–5084; *Angew. Chem.* **2019**, *131*, 5134–5138; g) R. Hahn, F. Bohle, W. Fang, A. Walther, S. Grimme, B. Esser, *J. Am. Chem. Soc.* **2018**, *140*, 17932–17944; h) K. I. Assaf, M. Florea, J. Antony, N. M. Henriksen, J. Yin, A. Hansen, Z. W. Qu, R. Sure, D. Klapstein, M. K. Gilson, S. Grimme, W. M. Nau, *J. Phys. Chem. B* **2017**, *121*, 11144–11162.

[53] a) O. Baud, S. Etter, M. Spreafico, L. Bordoli, T. Schwede, H. Vogel, H. Pick, *Biochemistry* **2011**, *50*, 843–853; b) K. Schmiedeberg, E. Shirokova, H. P. Weber, B. Schilling, W. Meyerhof, D. Krautwurst, *J. Structural Biol.* **2007**, *159*, 400–412.

[54] a) A. Suenaga, N. Okimoto, Y. Hirano, K. Fukui, *PLoS ONE* **2012**, *7*, e42846–e42846; b) P. Wang, T. Fu, X. Zhang, F. Yang, G. Zheng, W. Xue, Y. Chen, X. Yao, F. Zhu, *Biochim. Biophys. Acta: General Subjects* **2017**, *1861*, 2766–2777; c) K. Park, N. K. Sung, A. E. Cho, *Bull. Korean Chem. Soc.* **2013**, *34*, 545–548; d) T. Singh, O. A. Adekoya, B. Jayaram, *Mol. BioSyst.* **2015**, *11*, 1041–1051.

[55] a) M. Asakawa, Y. Fukutani, A. Savangsuksa, K. Noguchi, H. Matsunami, M. Yohda, *Sci. Rep.* **2017**, *7*, 10167; b) A. Robert-Hazotte, P. Faure, F. Neiers, C. Potin, Y. Artur, G. Coureaud, J.-M. Heydel, *Sci. Rep.* **2019**, *9*, 3104; c) A. Robert-Hazotte, R. Schoumacker, E. Semon, L. Briand, E. Guichard, J.-L. Le Quéré, P. Faure, J.-M. Heydel, *Sci. Rep.* **2019**, *9*, 2492; d) J.-M. Heydel, F. Menetrier, C. Belloir, F. Canon, P. Faure, F. Lirussi, E. Chavanne, J.-M. Saliou, Y. Artur, M.-C. Canivenc-Lavier, L. Briand, F. Neiers, *PLoS ONE* **2019**, *14*, e0220259.

[56] M. Wolfsberg, W. A. Van Hook, P. Paneth, L. P. N. Rebelo, *Isotope Effects in the Chemical, Geological, and Bio Sciences*, Springer, Dordrecht, **2010**.

[57] M. Na, M. T. Liu, M. Q. Nguyen, K. Ryan, *ACS Chem. Neurosci.* **2019**, *10*, 552–562.

[58] B. Malnic, D. C. Gonzalez-Kristeller, L. M. Gutiyama, *Odorant Receptors* (Ed.: A. Menini), CRC, Boca Raton, **2010**, pp. 181–202.

[59] J. Gunschera, F. Fuhrmann, T. Salthammer, A. Schulze, E. Uhde, *Environ. Sci. Pollut. Res.* **2004**, *11*, 147–151.

[60] N. Armanino, J. Charpentier, F. Flachsmann, A. Goeke, M. Liniger, P. Kraft, *Angew. Chem. Int. Ed.* **2020**, *59*, 16310–16344; *Angew. Chem.* **2020**, *132*, 16450–16487.

[61] ISO 16000–9, Indoor Air—Part 9: Determination of the emission of volatile organic compounds from building products and furnishing: Emission test chamber method, Beuth, Berlin, **2006**.

[62] J. Bartsch, E. Uhde, T. Salthammer, *Anal. Chim. Acta* **2016**, *904*, 98–106.

[63] A. T. Blades, *Can. J. Chem.* **1976**, *54*, 2919–2924.

[64] T. Holm, *J. Chromatogr. A* **1997**, *782*, 81–86.

[65] G. Bronner, K. Fenner, K.-U. Goss, *Fluid Phase Equilibria* **2010**, *299*, 207–215.

[66] K.-U. Goss, *Forensic Sci. Int.* **2019**, *296*, 110–114.

[67] a) C. Bannwarth, S. Ehlert, S. Grimme, *J. Chem. Theory Computation* **2019**, *15*, 1652–1671; b) C. Bannwarth, E. Caldeweyher, S. Ehlert, A. Hansen, P. Pracht, J. Seibert, S. Spicher, S. Grimme, *WIREs Comput. Mol. Sci.* **2020**, e01493, https://doi.org/10.1002/wcms.1493.

[68] Semiempirical extended tight-binding program package xtb" https://github.com/grimme-lab/xtb. Accessed: 2019, 12, 01.

[69] F. Neese, *WIREs Comput. Mol. Sci.* **2012**, *2*, 73–78.

[70] J. G. Brandenburg, C. Bannwarth, A. Hansen, S. Grimme, *J. Chem. Phys.* **2018**, *148*, 064104–064104.

[71] S. Grimme, *Chem. Eur. J.* **2012**, *18*, 9955–9964.

[72] R. Z. Liao, P. Georgieva, J. G. Yu, F. Himo, *Biochemistry* **2011**, *50*, 1505–1513.

[73] L. Goerigk, A. Hansen, C. Bauer, S. Ehrlich, A. Najibi, S. Grimme, *Phys. Chem. Chem. Phys.* **2017**, *19*, 32184–32215.

[74] S. Grimme, C. Bannwarth, E. Caldeweyher, J. Pisarek, A. Hansen, *J. Chem. Phys.* **2017**, *147*, 161708–161708.

[75] P. Pracht, F. Bohle, S. Grimme, *Phys. Chem. Chem. Phys.* **2020**, *22*, 7169–7192.

[76] K. Palczewski, T. Kumasaka, T. Hori, C. A. Behnke, H. Motoshima, B. A. Fox, I. Le Trong, D. C. Teller, T. Okada, R. E. Stenkamp, M. Yamamoto, M. Miyano, *Science* **2000**, *289*, 739–745.

[77] H. M. Berman, J. Westbrook, Z. Feng, G. Gilliland, T. N. Bhat, H. Weissig, I. N. Shindyalov, P. E. Bourne, *Nucleic Acids Res.* **2000**, *28*, 235–242.

[78] a) S. Schrödinger Release 2016–2: Schrödinger Suite 2016–2 Protein Preparation Wizard; Epik version 3.6, LLC, New York, NY, 2016; Impact version 7.1, Schrödinger, LLC, New York, NY, 2016; Prime version 4.4, Schrödinger, LLC, New York, NY, **2016**; b) G. Madhavi Sastry, M. Adzhigirey, T. Day, R. Annabhimoju, W. Sherman, *J. Comp. Aided Mol. Design* **2013**, *27*, 221–234.